Emerging approaches to study cell-cell interactions

Poulcharidis, D.

3

A flow cytometry assay to quantify intercellular exchange of membrane components

Published as part of: Dimitrios Poulcharidis, Kimberley Belfor, Alexander Kros and Sander I. van Kasteren. Chemical Science, *2017, 8, 5585-5590*

3.1 Introduction

The ability of cells to communicate with one another is one of the most important characteristics of eukaryotic and prokaryotic cells.[1,2] Some of this communication occurs by exchange of soluble cellular components between cells, such as peptides, larger proteins, individual amino acids and nucleotides,[2] by exosome secretion,[3] or through direct exchange of membrane components upon contact between cells.[4] This direct exchange of cellular components between neighbouring eukaryotic cells remains poorly described and its

involvement in cell-cell communication between neighbouring cells requires further study.[5]

Many cell wall components are not under direct genetic control. For example, in model systems, radiolabelled or fluorescently labelled cholesterol has been shown to exchange intracellularly between organelles[6] and liposomes[7] as well as between serum and erythrocytes.[8] The rate of lipid exchange in liposomes varies depending on the solubility, the acyl-chain, the length of the fatty acid and the hydrophobicity.[7,9,10] For example, most phosphatidylcholines (PtdCho) in cells with 16 or more carbon acyl chains have a transfer half-time of 83 hours.[9–11] On the other hand, 25-hydroxylcholesterol (25OH) is more hydrophilic than cholesterol and therefore exchanges more rapidly,[9,12,13] whereas cholesteryl oleate is more hydrophobic than cholesterol and exchanges more slowly.[9] Exchange of cholesterol between host cells and bacteria (i.e. *Borrelia burgdorferi*) was also recently reported to be an important process in the pathogenesis or infectivity of pathogens.[14]

Aside from these examples of cholesterol exchange, the study of membrane component exchange is relatively underexplored,[15,16] especially in mammalian cell systems. The dynamics and kinetics of membrane compound exchange critically impacts many different biological activities in cells including cell-cell recognition, energy production, signal transduction and conversion, cell adhesion and foreign molecule identification.[17,18]

Here an adaptable strategy utilising flow cytometry is presented, in which labelled membrane components are used to quantify their exchange rates (Scheme 1) between mammalian cells in co-culture, quantify the interactions between glycans and membrane lipids, and

understand the exchange mechanism. This approach is then applied to study the exchange of fluorescently labelled cholesterol,[19] alkyne-modified cholesterol[20] as well as azide-modified sialic acids to determine any differences in exchange between these different classes of membrane components.[21] The latter two are visualised in a two-step bioorthogonal method.[22,23] Using this approach, the rate of sterol exchange was shown to be highly cell-line dependent and the rate of sialic acid-containing component exchange is significantly slower than that of the sterolic lipids. Finally, a non-exchanging cell line was forced to exchange both sterols and carbohydrates when brought into prolonged close proximity using complementary coiled-coils.[24,25] This suggests that lipid exchange mediated by direct contact is the dominant mechanism of sterol exchange in these cells.

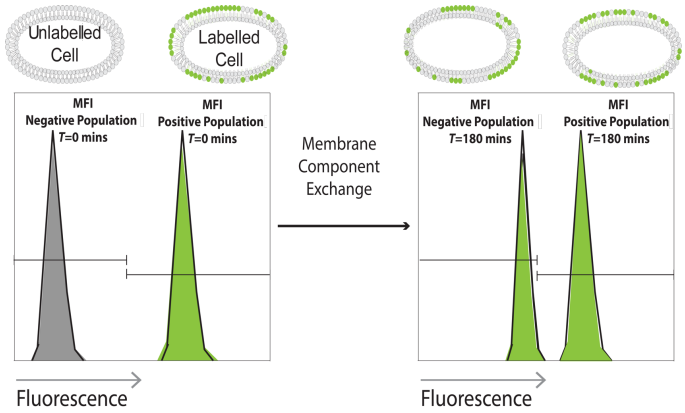

Scheme 1 *Schematic overview of the approach: cell lines are treated with fluorescently labelled sterol and/or glycan and co-cultured with analogous untreated cells. Analysis by flow cytometry over time shows the rate of exchange of the fluorescent membrane component to the non-fluorescent population as a shift in mean fluorescent intensity (MFI).*

3.2 Results and discussion

The initial aim was to develop a broadly deployable assay that would allow the facile quantification and mechanistic characterisation of the exchange of membrane components between cells by flow cytometry (Scheme 1). The recently reported bodipy-modified cholesterol

(1, Scheme 2), which readily inserts into eukaryotic cell membranes, was used to determine whether this exchange could be visualised (Figure 1).[19]

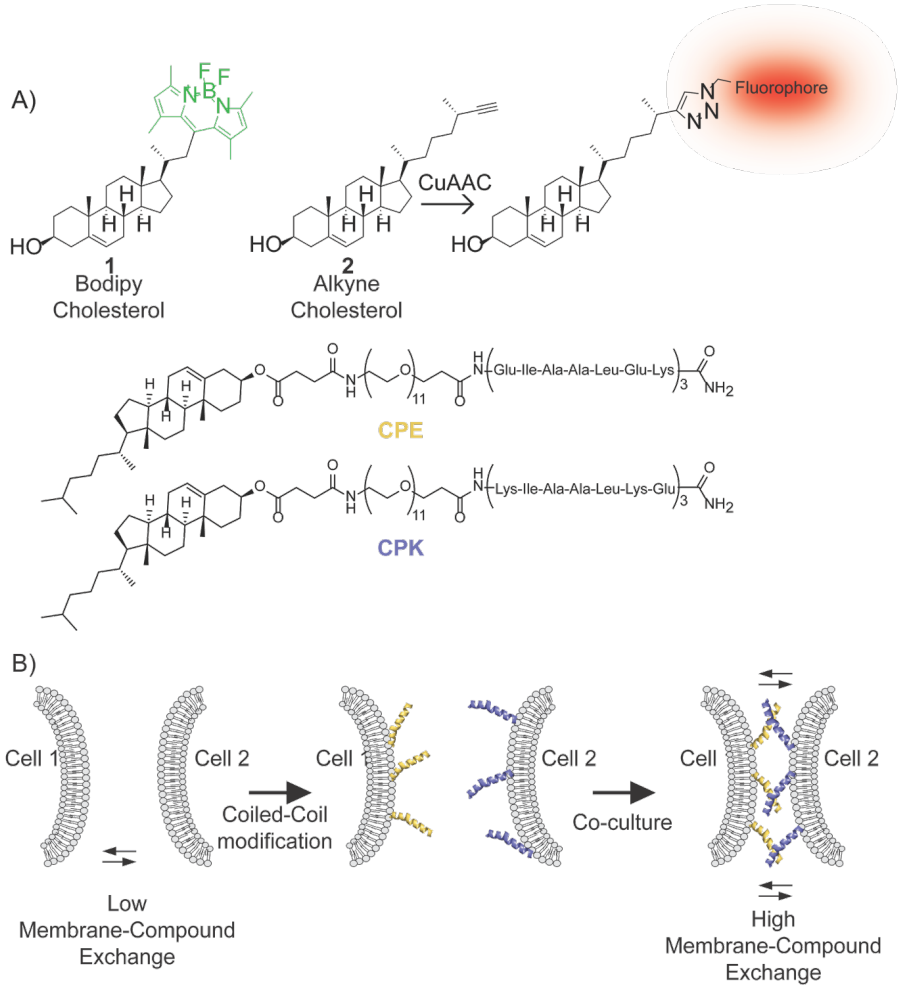

Scheme 2 *(A) Structures of bodipy-cholesterol (Bdp-Ch,* ***1****), alkyne-cholesterol (Alk-Ch,* ***2****), cholesterol modified* E_3 *(CPE) and* K_3 *(CPK) peptides. (B) Schematic representation of coiled-coil formation and its use to prolong cell-cell contact thus enhancing membrane compound exchange.*

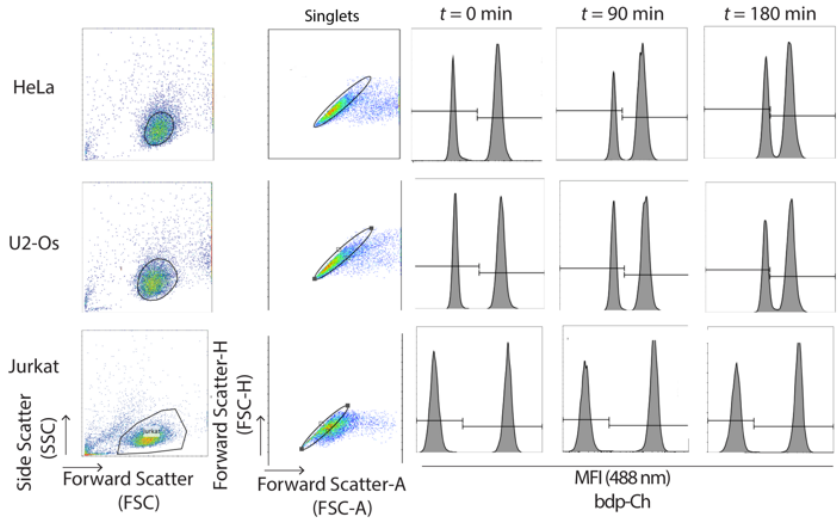

Figure 1 *The flow cytometry assay indicates cholesterol exchange between live HeLa and U2-Os cells, whereas no exchange occurs between Jurkat cells. Cells were treated with 5 μM bdp-Cholesterol (1, Scheme 1) for 18 h. Labelled and unlabelled live cells were co-cultured and flow cytometry was completed. The cell population was gated based on FSC-A vs. SSC-A (cell doublets were gated out using FSC-H vs. FSC-A) and histograms of mixed cells; t = 0, 90 and 180 mins are shown for each cell line with mean fluorescent intensity (MFI) gated accordingly.*

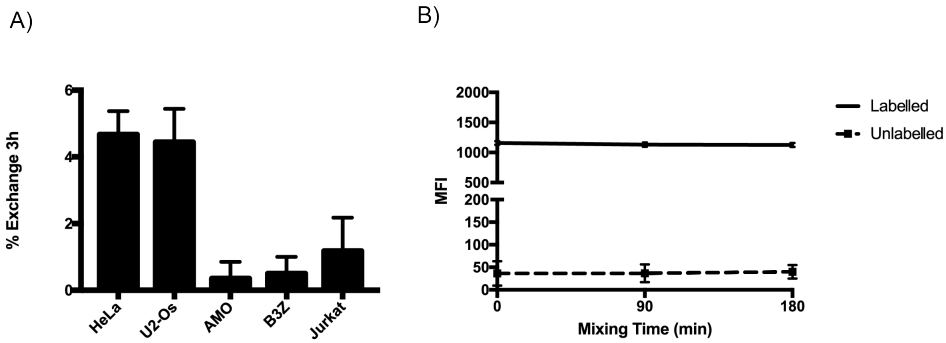

Figure 2 *Exchange rates of bodipy cholesterol (bdp-Ch 1) are cell-type and live-cell dependent. Cells were incubated overnight with bodipy cholesterol and then mixed with unlabelled cells for 3 h. Flow cytometry results were analysed and showed differences in the lipid exchange rates for the different cell lines. (A) Expression of fluorescent signal exchange after 3 h for different cell lines indicating that the lipid exchange depends on the cell line. (B) Fixation abolished lipid exchange of HeLa cells; HeLa cells fixed using 2% PFA for 15 mins prior to co-culture. Data are represented as mean ± SD. Error bars SD.*

To study whether exchange of this lipid could be observed, various cell lines (HeLa,[26] U2-Os,[27] Jurkat,[28] AMO,[29] and the B3Z T cell[30]) were incubated with **1** as described.[19] Unlabelled cells were then mixed with labelled cells and co-cultured at 37 °C for different times. The amount of exchange of the fluorescently labelled cholesterol over time between these two populations was then determined using flow cytometry (Figure 1 and Figure 2A). In this assay, the rate of exchange of bodipy cholesterol (bdp-Ch 1) was shown to vary significantly between the different cell lines: after three hours HeLa and U2-Os had exchanged 4.5 ± 0.17% and 4.4 ± 0.05% of 1 respectively. Jurkat, AMO and B3Z cells on the other hand had exchanged < 1% (0.9 ± 0.23%, 0.4 ± 0.03% and 0.6 ± 0.12% respectively) (Figure 3A and Figure 3B). It was hypothesized that cell-cell contact might be the driving force for membrane lipid exchange as no exchange between suspension cell lines – which have limited cell-cell contact – was observed. The rate of exchange (% exchange, ΔMFI, eq 1) was normalised to live cells based on scatter plots and cellular fluorescence. The ΔMFI was calculated as the amount of fluorescent intensity the unlabelled (negative) cells gained at time t = 180 mins of co-culture with labelled (positive) cells in correlation with the total fluorescent intensity (the initial fluorescently labelled cell population) (eq 1).

$$\Delta MFI = \frac{MFI_{\text{negative } (t = 180 \text{ mins})} - MFI_{\text{negative}(t=0 \text{ mins})}}{MFI_{\text{positive } (t=0 \text{ mins})}} \qquad \text{(eq 1)}$$

Here, flow cytometry was used to determine the differences in cholesterol exchange between live HeLa cells as a function of lipid concentrations. Cells were treated with bodipy-modified cholesterol (bdp-Ch, 1; 1 μM, 5 μM and 10 μM) for 18 hours before mixing with unlabelled live cells. Upon flow cytometry analysis, the cell

populations were gated based on forward scatter area (FSC-A) and side scatter area (SSC-A) characteristics (cell doublets were gated out using FSC-A vs. FSC-H). An increase in the percentage of a new-labelled cell population and a decrease in the number of unlabelled cells was observed, indicating that rate of exchange of cholesterol 1 is concentration dependent (Figure 3C).

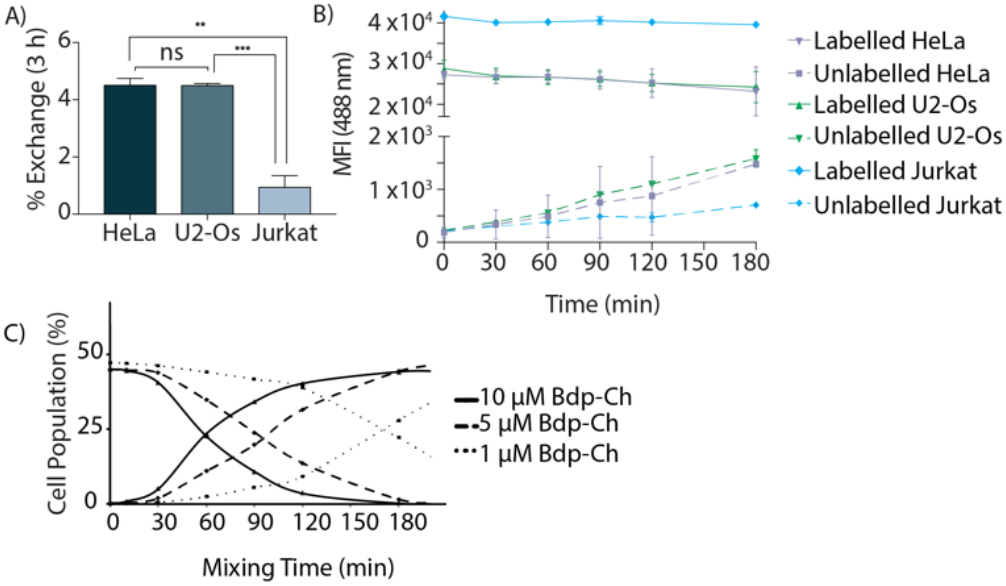

Figure 3 *(A) The percentage exchange or ΔMFI of the fluorescent signal exchange after 3 h co-culturing was calculated using ΔMFI = (MFInegative(t = 180 mins) − MFInegative(t = 0 mins))/MFIpositive(t = 0 mins). Data are represented as mean ± SD. Error bars SD; *p < 0.05; **p < 0.01; ***p < 0.001; ns = not significant; unpaired t-tests. (B) Mean fluorescent intensity (MFI) of labelled and unlabelled cells over varied co-culturing time periods. Data are represented as mean ± SD. Error bars SD. (C) Cholesterol exchange is concentration dependent. In live HeLa cells, the amount of co-culturing time for 25% of the unlabelled population to get labelled varies significantly under different lipid concentrations. Cells were treated with 1 µM, 5 µM or 10 µM bdp-Ch 1 for 18 h prior to co-culturing with unlabelled live cells.*

In order to study that the observed exchange rates were not due to the fluorescent label, unmodified bodipy-488 was used as a control and, as expected, did not exchange (Figure 4), showing that the sterol moiety is essential for the exchange reaction. Altering the ratio of labelled vs. unlabelled cells (1:1, 1:5, 1:10) and vice versa, or increasing the culture volume, also affected the rate of exchange (Figure 5), showing that close contact is necessary for the membrane compound exchange. It was found that the higher the fraction of labelled cells, the faster the exchange: 1:1 ratio exchanged 19 times faster than a 1:10 ratio of labelled vs. unlabelled cells (3.9 ± 0.5% vs. 0.2 ± 0.05%; Figure 5).

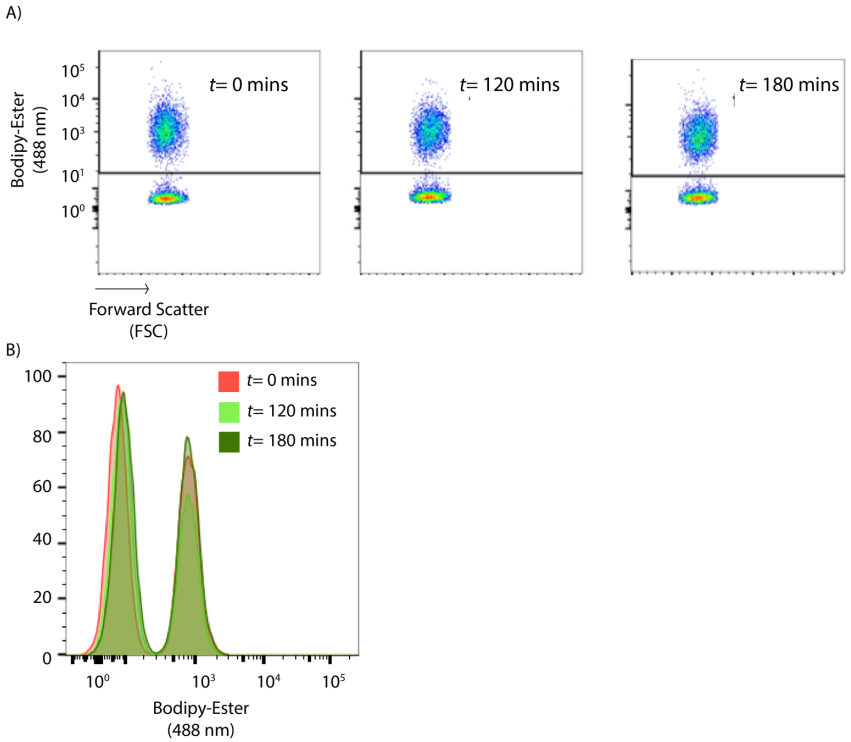

Figure 4 *Exchange of bodipy-488. Flow cytometry assay indicates no bodipy is exchanged between labelled and unlabelled HeLa-cells. Cells treated with bodipy-ester (5 µM for 24 h) were mixed with unlabelled HeLa cells. (A) Scatter plots and (B) overlay histograms of mixing experiments (t=0, 120 and 180 mins) showing any shift.*

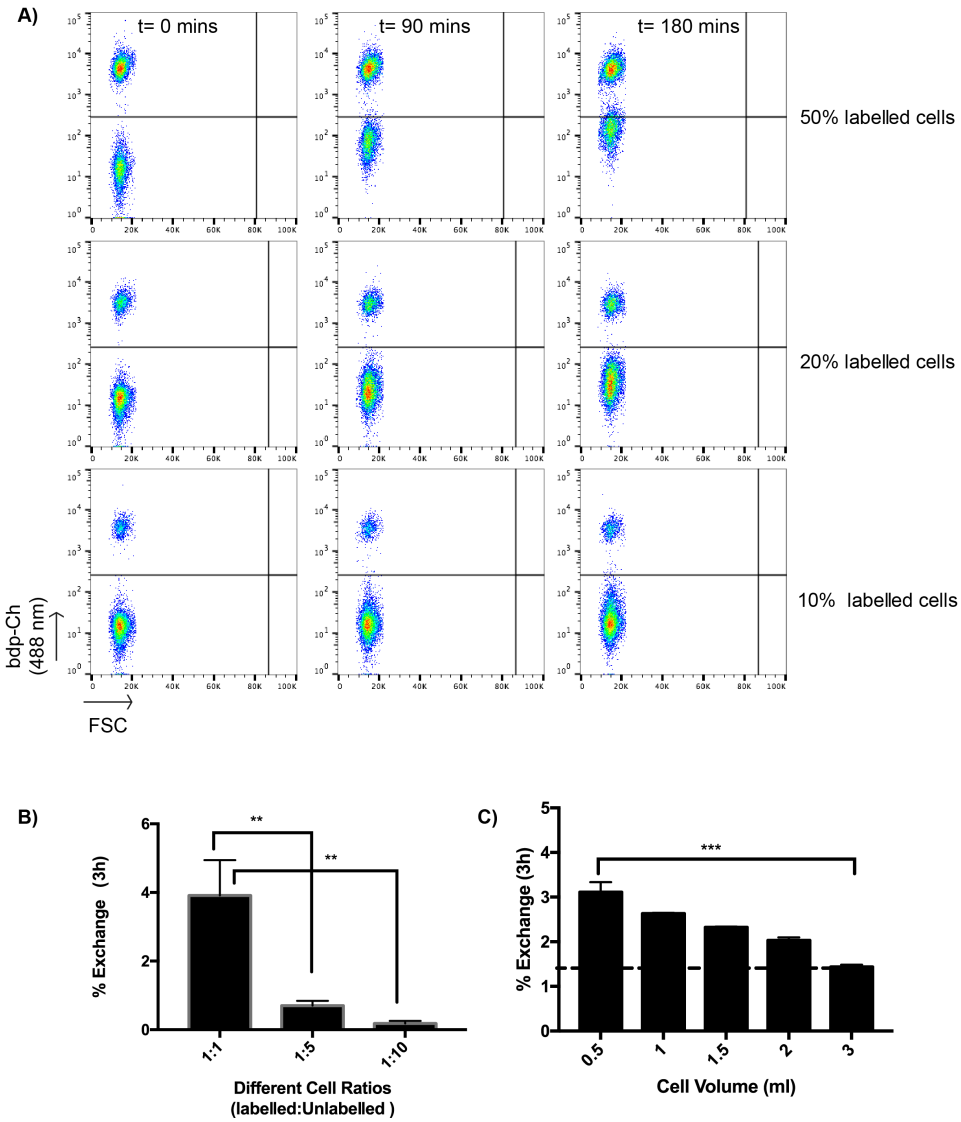

Figure 5 *Cell ratios affect cholesterol exchange: HeLa cells were mixed at either different ratio of labelled vs. unlabelled cells (1:1, 1:5, 1:10) or different culture volume. (A, B) Flow cytometry analysis (t=60, 90, 180 mins) shows exchange rates to be dependent on fluorescent cell fraction. I Flow cytometry analysis after 180 mins showed rated to be dependent on the culture media volume. Data are representing as mean ± SD. Error bars SD; *p<0.05; **p<0.01; ***p<0.001; unpaired t-tests.*

In order to exclude the possibility that the observed cholesterol exchange was due to endocytosis of cell debris, passive uptake from dead cells or exosomes, and rather due to a live-cell dependent process, a series of different control experiments was performed. Cell death was first quantified in the co-culture experiments, by adding membrane impermeable propidium iodide (PI) dye[31] to the cell co-cultures prior to flow cytometry assay showing that the number of dead cells was always <2% (Figure 6B and Figure 6C), even when low temperature or sodium azide were used. In case of fixed cells, a fixable viability dye for live/dead selection could be used instead. Then, in order to exclude the possibility that the observed cholesterol exchange was due to endocytosis of cell debris, unlabelled cells were co-cultured with the lysate from cells labelled with **1**. In this system, there was no lipid uptake or fluorescent labelling after three hours (Figure 6A) at a lysate concentration representing 5% dead cells. Hypothermia or metabolic inhibitors (such as sodium azide) have a major impact in energy-dependent metabolic or biological processes.[32–34] Moreover, when cells were co-cultured under these conditions, differences in the number of dead cells could not be observed (Figure 6B and Figure 6C). Upon ATP depletion with sodium azide or low temperature, membrane lipid exchange was minimised or abolished respectively, indicating that the cholesterol exchange is energy dependent (Figure 6D). Using a chemical fixation step, biological, biochemical and proteolytic processes could be inactivated and cellular components could be kept immobilised and as 'lifelike' as possible.[35,36] Consequently, paraformaldehyde-fixation prior to mixing abolished all exchange (Figure 2B) indicating that the lipid exchange is a live-cell dependent process.

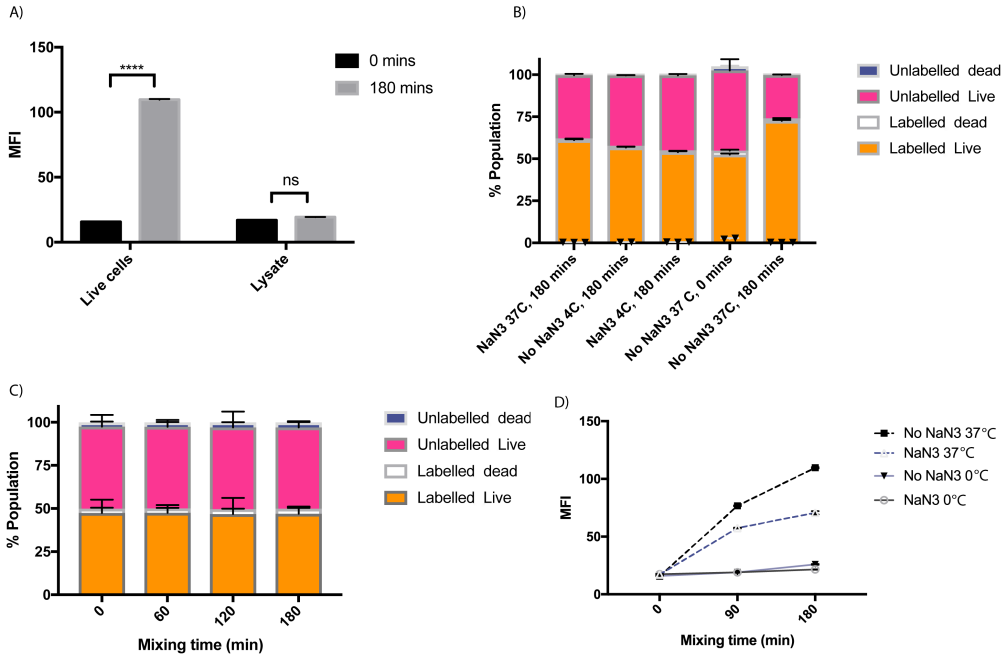

Figure 6 *Cell debris does not affect the lipid exchange in HeLa cells. (A) Labelled HeLa cells with bdp-Ch 1 were lysed by ultra-sonication and co-cultured with unlabelled cells at 37 °C for 3 h. MFI was calculated using flow cytometry and results showed any uptake of the fluorescent lipid difference. (B) Labelled HeLa-cells with bdp-Ch 1 were co-cultured for 3 h with unlabelled cells with or without 1 mM sodium azide at 37 °C or 4 °C. Propidium iodide (PI) used as live/dead dye. Flow cytometry analysis indicates <2% cell debris and lipid exchange independent of cell debris and only at 37 °C. (C) Labelled HeLa-cells with bdp-Ch 1 were co-cultured with unlabelled cells with 1 mM sodium azide at 4 °C for metabolic and energetic inhibition; flow cytometry analysis indicates <2% cell debris, the absence of toxicity during these conditions and the absence of lipid exchange due to cell debris. (D) Cellular energy is necessary for membrane lipid exchange. Labelled HeLa-cells with bdp-Ch 1 were co-cultured with unlabelled cells with 1 mM sodium azide for ATP depletion at 37 °C or 4 °C. Flow cytometry analysis indicates the absence of lipid exchange at 4 °C or the decrease of the exchange at 37 °C with sodium azide.*

To study whether the mechanism of exchange was based on the exchange of exosomes, the exchange of free **1** or cell-cell contact, unlabelled and labelled populations have been spatially separated in a trans-well assay (Figure 7A).[37] All sterol exchange was abolished,

even when large-pore (0.4 μm) membranes were used (through which exosomes can pass and cells cannot[38]), indicating that cell-cell contact is most likely responsible for the exchange of **1**. The absence of any incorporation of **1** in unlabelled cells after a supernatant transfer from a labelled population (Figure 7B) strongly supports the hypothesis that cell-cell contact is the main method of exchange of cholesterol in this system.

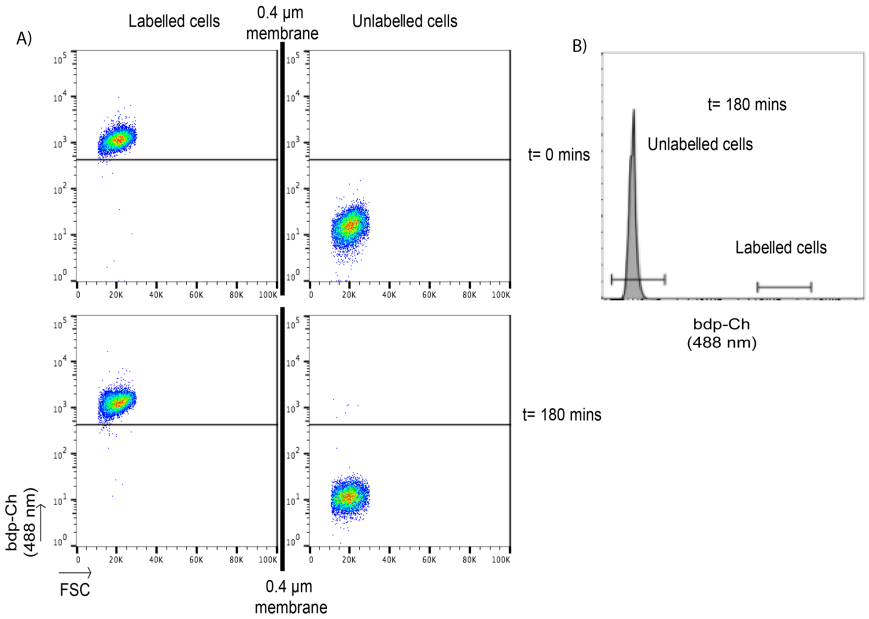

Figure 7 *HeLa cells show no lipid exchange when co-cultured in a trans-well plate. (A) Labelled HeLa-cells with bdp-Ch* ***1*** *were separated by a 0.4 µm membrane from unlabelled cells and incubated for 3 h. Flow cytometry analysis indicates the absence of lipid exchange. (B) Supernatant exchange. HeLa-cells were incubated with 1) and washed with PBS. After 1 h, the supernatant was collected and added to an unlabelled population of HeLa-cells for 3 h. No labelling was observed.*

To further investigate that close contact between cells is important for lipid transfer, testing was done as to whether forcing the cells into prolonged close proximity would enhance the exchange rate. A supramolecular approach was chosen, by which a pair of

complementary lipidated coiled-coil peptides was introduced[24,25] to force cells in close proximity in a non-covalent manner (Scheme 2, Figure 8). Coiled-coil-forming peptides E [$(EIAALEK)_3$] and K [$(KIAALKE)_3$] conjugated via a poly(ethylene glycol)$_{12}$ spacer with a cholesterol moiety (denoted CPE or CPK respectively) have been reported to insert spontaneously into cell membranes,[39–44] and were used here to study lipid exchange.

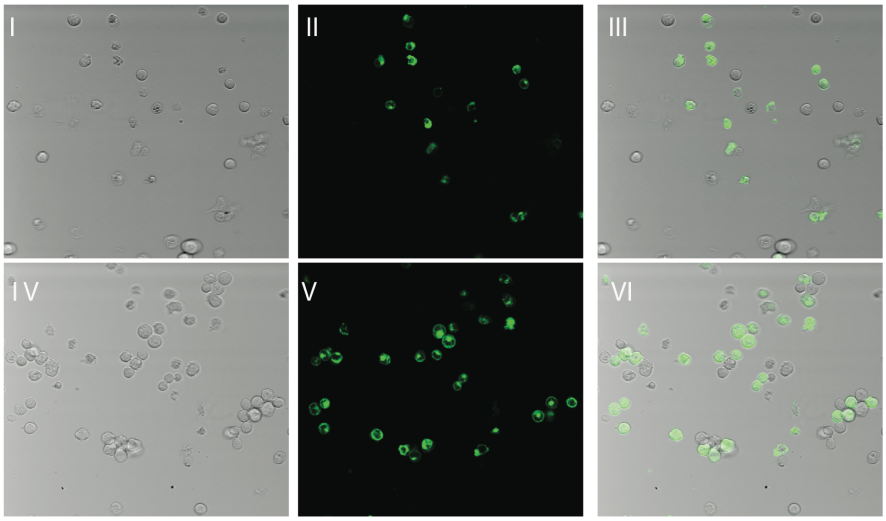

Figure 8 *Confocal microscopy of Jurkat cells with or without coiled coil. (I-III) Jurkat cells were labelled with 1 and co-cultured with unlabelled cells without the presence of lipidated coiled-coil peptides. (IV-VI) Jurkat cells were labelled with 1 and treated with 5 μM CPE and were co-cultured with unlabelled cells which had been pre-treated with 5 μM CPK.*

To study the effect of forced proximity on cholesterol exchange, lymphocytic Jurkat cells were used as these showed the lowest exchange rate (Figure 3A). The cells were labelled overnight with **1** and after washing were incubated with 5 μM cholesterol-CPE. In parallel, unlabelled cells were treated with 5 μM CPK. Next, the CPE- and CPK-modified Jurkat cells were mixed and the rate of exchange of 1 was determined. Flow cytometry results indicate that upon coiled-coil

formation between CPE- and CPK-modified cells, membrane-cholesterol exchange was enhanced 3-fold (from 1.0 ± 0.18% to 3.3 ± 0.35%) compared to coiled-coil peptide untreated cells (Figure 9A and 9B). The results are suggestive of the exchange rate of **1** being enhanced by forced membrane contact (Figure 9C). Moreover, confocal microscopy after three hours confirmed that upon coiled-coil formation, cells were in close proximity (Figure 8).

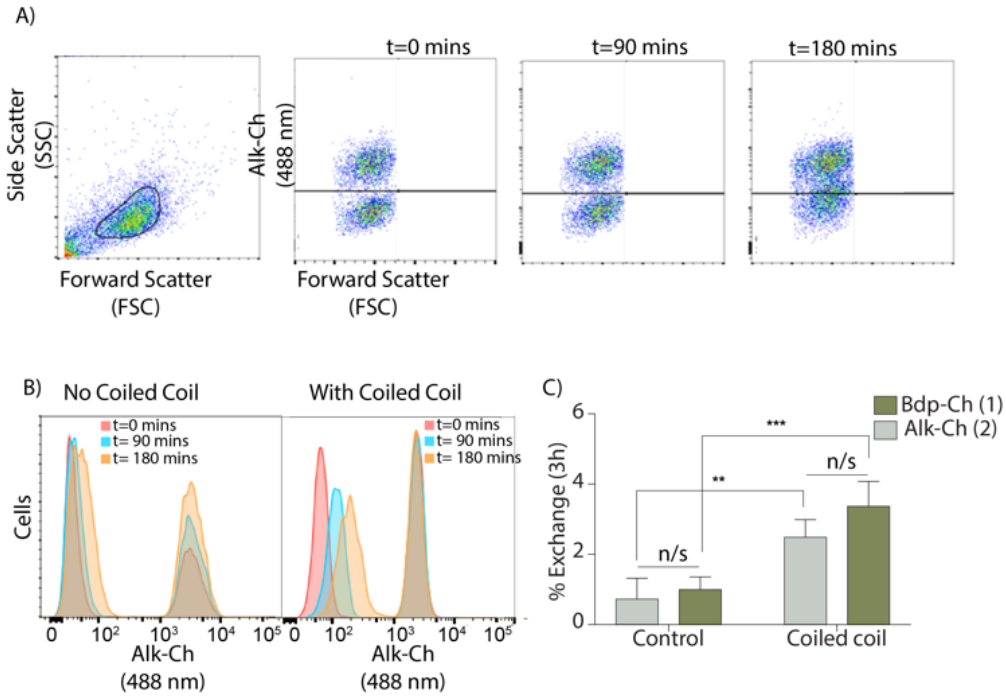

Figure 9 *(A) Forcing cells in close proximity using lipidated coiled-coil (CC) peptides enhances sterol exchange. The first dot-plot shows the gated cell population followed by three dot-plots showing the coalescence of the labelled and unlabelled cells using Alk-Ch (**2**) at t = 0, 90 and 180 mins. (B) Histograms of Jurkat cells over different co-culturing times using alk-Ch (**2,** Avanti) with and without coiled-coil peptides. (C) Exchange rates of **1** and **2** in Jurkat cells after 3 h co-culturing in the presence or absence of CC peptides. Both **1** and **2** show similar exchange rates between CC- and non-CC-labelled cell populations. Data are represented as mean ± SD. Error bars SD; *p < 0.05; **p < 0.01; ***p < 0.001; unpaired t-tests.*

Many membrane components are not amenable to selective fluorophore labelling and the bulky nature of such groups can affect the biological properties of the parent molecule. After establishing the exchange rate of fluorophore-modified cholesterol **1** between different cell types and manipulating these rates of exchange through forcing cell-cell contacts, the cytometry analysis was combined with the detection of bioorthogonal groups in a two-step approach to monitor the exchange of other membrane components.[45]

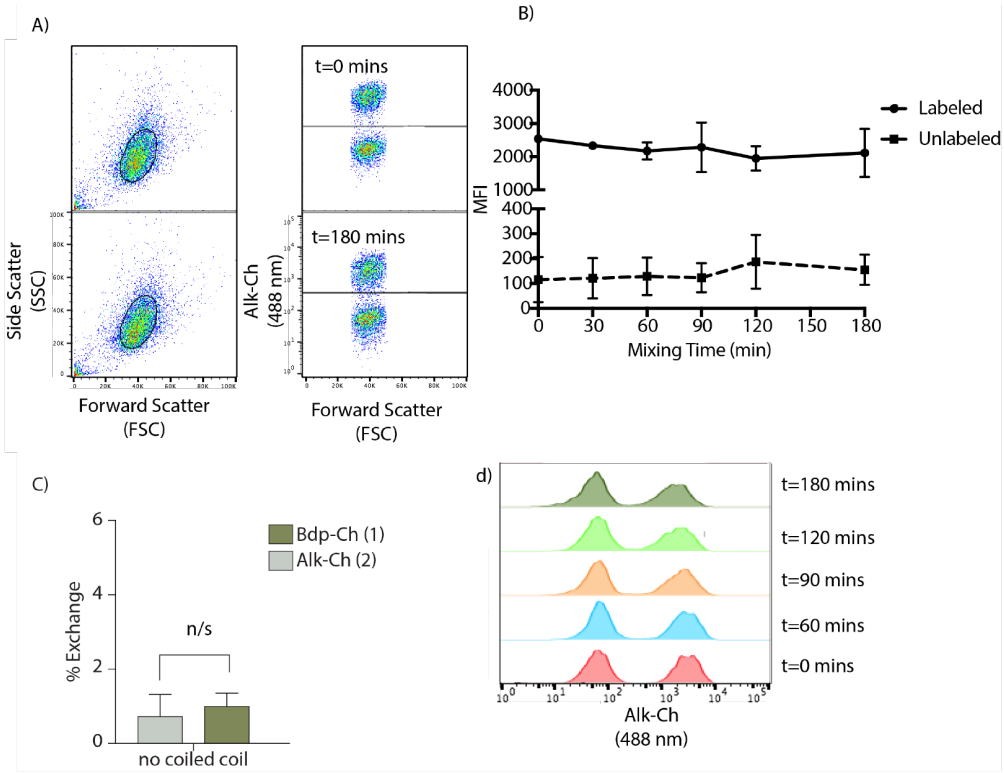

Figure 10 *Flow cytometry assay indicates no cholesterol exchange between live Jurkat cells. Cells were treated with cholesterol-alkyne (Alk-Ch 2, Avanti, 10 μM for 24 h). Labelled and unlabelled live cells mixed and labelled using copper-catalysed azide-alkyne cycloaddition (CuAAC) and flow cytometry assay showed any cholesterol exchange. (A) Dot plots and histograms of mixing cells at t=0 mins and t=180 mins. (B) MFI in different times. (C) Exchange rates of Alk-Ch (2) and bdp-Ch (1) in Jurkat cells in the absence of CC peptides. (D) Histograms in different times, showing no Alk-Ch (2) exchange. Data are represented as mean ± SD. Error bars SD.*

Bioorthogonal chemistry can be used to visualise non-genetically templated biomolecules in cells by means of incorporating a small biologically inert chemical group into a biomolecule class of choice and visualising these at the end of an experiment using tag-selective ligation chemistry.[22,23] The main advantage of this approach is that the small and stable bioorthogonal groups can be incorporated into non-templated molecules and can then hijack the biosynthetic pathways of these molecules. This approach has been used extensively to label many different cell biomolecules, such as glycans, lipids and nucleotides.[46,47] To determine whether a two-step bioorthogonal approach could be used to measure exchange kinetics, first the approach was validated using the recently reported alkyne-modified cholesterol **2**.[20] In a coiled-coil-enhanced exchange experiment in non-adherent Jurkat cells, a comparable 2.5-fold increase in the exchange rate with and without coiled-coil treatment was observed (from 0.7 ± 0.30% without CC to 2.5 ±0.25% with CC after three hours; Figure 9, Figure 10). For this experiment, live-cell compatible variants of the copper-catalysed azide-alkyne cycloaddition (CuAAC) were initially used.[48]

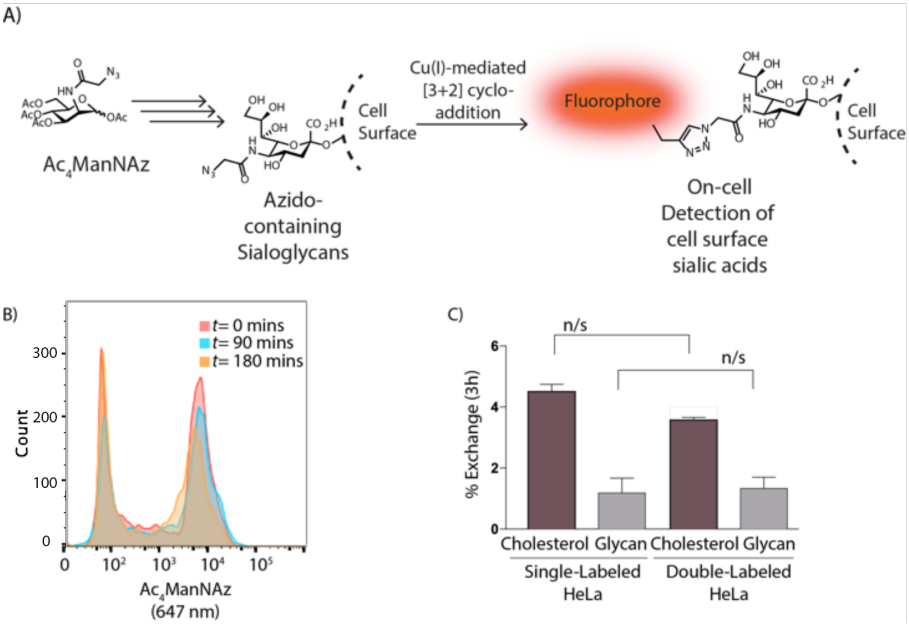

Figure 11 *(A) Schematic representation of cell surface glycan labelling. (B) Flow cytometry overlay histograms on different times show no enhancement of glycolipid exchange between Jurkat cells after coiled-coil formation; Jurkat cells were treated with Ac4ManNAz and CPE co-cultured with untreated cells with CPK and labelled with CuAAC. (C) ΔMFI [ΔMFI= ($MFI_{negative\ (180\ mins)}$-$MFI_{negative\ (0\ mins)}$ / $MFI_{positive\ (0mins)}$] expression of exchange after 3 h between sterol and glycan in single- and double-labelled co-culture experiments; data show lipid exchange independently of the glycan exchange. Data are represented as mean ± SD. Error bars SD; n/s p > 0.05; unpaired t-tests.*

Based on previously reported evidence that by using lower copper concentrations in combination with chelating ligands (TTMA, THPTA, BTTAA, etc.) toxicity could be minimised and be equally "non-toxic" with strain-promoted cycloadditions, [49–51] the conditions were optimised using the well-established WST-1 viability assay. However, despite the fact that these conditions did not significantly affect cell viability as measured by WST-1 viability assay and also 7-AAD (7-Aminoactinomycin D) viability dye (Figure 13), the cells displayed aberrant morphology as determined by flow cytometry (Figure 12). One explanation for this aberrant morphology could be that under

these conditions programmed cell death had commenced. Therefore, a fix-and-click protocol was used in which the cells were first paraformaldehyde-fixed (2%) prior to CuAAC labelling.[36,52] In flow cytometry, a cell traverses through a laser beam allowing the instrument to measure the amount of light which goes around the cell or cell size (FSC) and the amount of light which bounces off the internal particulates of a cell or cell granularity (SSC).[36,53] The ce'l's ability to scatter light is altered during cell death, reflecting morphological changes such as cell swelling or shrinkage.[53] Therefore changes in morphology of a dying cell can be detected using light scatter in flow cytometry.

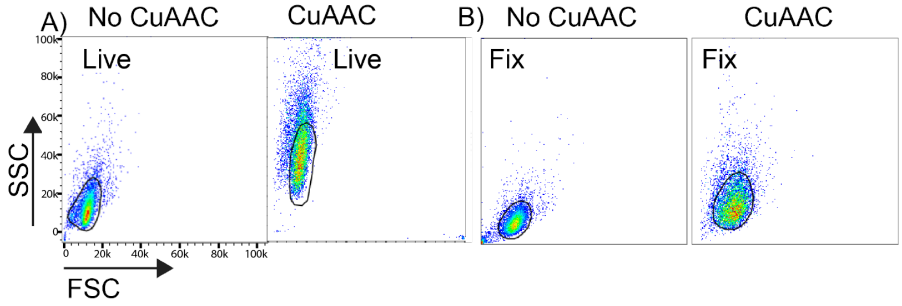

Figure 12 *Live-cell CuAAC affects cellular morphology. HeLa-cells treated with cholesterol-alkyne were subjected to CuAAC conditions with Alexa Fluor® 488 azide. (A) FSC/SSC before addition of CuAAC-reagent mix of unfixed and fixed cells. (B) FSC/SSC after addition of reagents to unfixed and fixed cells. Fixed cells retain their FSC/SSC profile, whereas live cells broaden their FSC/SSC value distribution.*

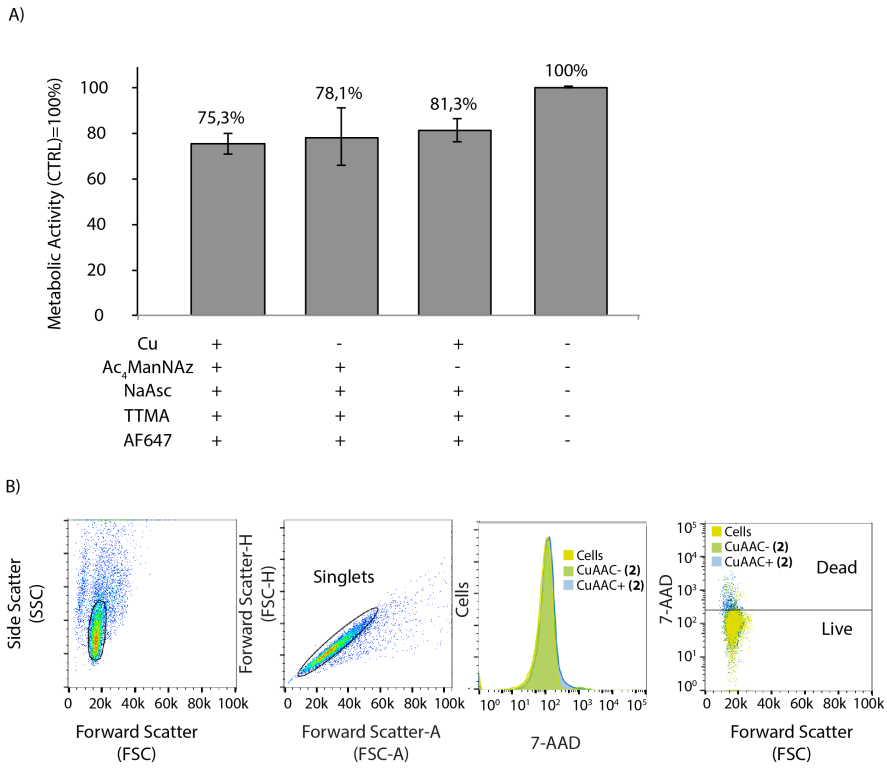

Figure 13 *CuAAC does not have a major impact in cell viability. (A) Cells were treated with/without Ac4ManNAz for 72 h or with Alk-Ch (2, Avanti) 10 uM, and then subjected to CuAAC (with or without catalyst) conditions for 5 mins (100 µM CuSO4, 250 µM TTMA [(Tris((1-((O-ethyl)carboxymethyl)-(1,2,3-triazol-4-yl))methyl)amine] ligand, 2.5 mM sodium ascorbate and 3 µM Alexa Fluor® 647 Alkyne or Alexa Fluor® 488 azide). Cells were washed 3 times. The cell WST-1 viability assay[84] shows no difference in cell viability under these CuAAC conditions, despite the observed morphological changes in S10. (B) Cells treated with Alk-Ch (2, Avanti) 10 uM and were subjected to CuAAC; 7-AAD viability dye was used and no major cell toxicity (<4 %) was defined.*

Having established the suitability (and limitations) of a bioorthogonal approach to detect cholesterol exchange, a similar approach was used to determine whether the exchange of another integral membrane component could be monitored: sialoglyoproteins and sialoglycolipids. These vital membrane components have been associated with cell-cell communication, metastatic behaviour, human disease and cell recognition.[55] HeLa cells were first labelled using a

bioorthogonal analogue of the metabolic precursor of sialic acid, per-O-acetylated N-2-azidoacetylmannosamine (Ac_4ManNAz),[21] which is converted to sialic acid inside the cell and transferred to nascent galactose-terminated glycans in the trans-Golgi network (Figure 11A). Previously well-established protocols indicate that a sufficient amount of corresponding sialic acids is biosynthesised and presented in cell surfaces after three-day treatment with the specific metabolic sialic acid precursors.[50,56–58] Here, HeLa cells were treated with 50 μM Ac_4ManNAz for 72 hours prior to mixing and co-culturing with untreated HeLa cells. Flow cytometry after paraformaldehyde fixation (2%) showed that the rate of exchange of the sialoglycome was significantly slower (0.98 ±0.40% after three hours) compared to cholesterol exchange (Figure 11B and Figure 11C).

This lack of exchange was not due to the Ac_4ManNAz labelling, as the exchange of **1** in cells labelled with both Ac_4ManNAz and **1** was unaffected (Figure 11C). A speculation about the biological significance of the absence of exchange could be made: the observed slower exchange of glycans between cells may reflect reduced freedom of movement of these larger sialoglycolipids in the cell membrane, or their specific function in cell adhesion.[59-61]

3.3 Conclusions

This study demonstrates that different mammalian cells exchange membrane components in a time- and cell-type dependent manner. This exchange appears to be due to cell-cell contacts and can be enhanced when cells are forced in close proximity. The exchange of sialylated membrane components appears to be significantly slower compared to sterols, indicating the presence of differential control mechanisms of exchange for these components. Radio-labelled

cholesterol in combination with mass spectroscopy and targeted metabolomics could be used in later stages for validation of the aforementioned technique. These experiments could be used to study the exchange of other lipids as well, such as inflammatory mediators[62,63] and mediators of neuronal signaling[64,65] as these have been shown to be amenable to bioorthogonal or fluorescent modification[66]. This will likely help to improve understanding of the role of these compounds in cell-cell communication, cell interactions and disease development.

3.4 Experimental methods

Reagents

Cholesterol and all other chemical reagents were purchased at the highest grade available from Sigma-Aldrich and used without further purification. All solvents were purchased from Biosolve. Phosphate buffered saline (PBS) consisted of 5 mM KH_2PO_4, 15 mM K_2HPO_4, 150 mM NaCl, pH 7.4. Silica gel column chromatography was performed using silica gel grade 40-63 μm (Merck). Thin-layer chromatography (TLC) analysis was performed using aluminium-backed silica gel TLC plates (60_F 254, Merck), visualisation by UV absorption at 254 nm and/or staining with $KMnO_4$ solution. NMR spectra (^1H and ^{13}C) were measured on a Bruker AV-400MHz spectrometer at ambient temperature at the Leiden Institute of Chemistry NMR facility. Chemical shifts are recorded in ppm. Tetramethylsilane (TMS) is used as an internal standard. Multiplicity was reported as follows: s = singlet, d = doublet, dd = doublet of doublets, t = triplet, q = quartet, m = multiplet, br = broad. Electrospray LC-MS analysis was performed on a PE SCIEX: API 3000 LC/MS/MS system using a Gemini 3u C18 110A analytical column (5μ particle size, flow: 1.0 ml/mins), on which the absorbance was measured at 214

and 254 nm. Solvent system for LC-MS: A: 100% water, B: 100% acetonitrile, C: 1% trifluoroacetic acid (TFA) (aq). MALDI-TOF mass spectra were acquired using an Applied Biosystems Voyager System 6069 MALDI-TOF mass spectrometer. α-Cyano-4-hydroxycinnamic acid (CHCA) was used as matrix in all cases. Sample concentrations were ~0.3 mg/ml. HPLC-ELSD analysis was performed using a Shimadzu HPLC set-up equipped with two LC-8A series pumps coupled to a Shimadzu ELSD-LT II detection system. Separation (Vydac 214 MS C4 column, 5u, 100 × 4.6 mm, flow rate: 15 mL/mins), in all instances, was carried out over a linear gradient of 10-90% B over 20 minutes with an initial five-minute hold at 10% B. HPLC buffers: A: H_2O (0.1% TFA); B: acetonitrile (0.1% TFA). The drift tube temperature for ELSD was set at 37 °C and the nitrogen flow-rate at 3.5 bar.

Flow cytometry[36,53]

Flow cytometry assays were performed using the Merck Guava® easyCyte 12HT Benchtop Flow Cytometer and all flow cytometry data was analysed using FlowJo™ v10.1 (FlowJo, LLC). Counting and characterization was performed by measuring 10,000 events in triplicate and concatenation of this data. For manual gating, the outermost ring of the dot plot was selected. Quadrants were manually selected to illustrate fluorescence plots. No compensation was required.

Flow cytometry is a technology that simultaneously measures and then analyses multiple physical characteristics of single particles, usually cells, as they flow in a fluid stream through a beam of light. Light scattering occurs when a particle deflects incident laser light. Correlated measurements of forward-scattered light (FSC) and side-

scattered light (SSC) can allow for differentiation of cell types in a heterogeneous cell population. FSC is proportional to cell-surface area or size, whereas SSC is proportional to cell granularity or internal complexity

Cholesterol exchange assay

For the study of cholesterol exchange, cells were incubated with Bdp-Cholesterol 1 (TopFluor®, Avanti) for 18 hours at 37 °C. Cells were washed six times, before co-culture with unlabelled cells. For the study of exchange of adherent cells, the cells were detached prior to exchange using EDTA/PBS for 15 minutes and seeded in a 96-V-plate for the mixing and exchange.

Coiled-coil enhancement of exchange reaction

For the coiled-coil formation labelled cells were treated with 5 μM CPE and the unlabelled cells with 5 μM CPK for 10 minutes at 37 °C. Cells were washed twice with PBS and resuspended in fresh media. Cells were mixed and co-cultured for different time periods (20,000 cell/100μl treated+ 20000 cell/100μl untreated) in media with or without serum. Fluorescence was then measured using Guava® easyCyte 12HT Benchtop Flow Cytometer and results analysed using FlowJo™ v10.1 (FlowJo, LLC).

Bioorthogonal sialylated glycan exchange assay

For the glycan studies, cells were incubated with 50 μM Ac_4ManNAz for 72 hours at 37 °C. Adherent cells were detached using 2 mM EDTA/PBS for 15 minutes and mixed in a 96-V-plate with unlabelled cells. For the coiled-coil mediated exchange enhancement, cells were treated with 5 μM CPE and 5 μM CPK for 10 minutes at 37 °C prior to mixing. Cells were washed twice with PBS and resuspended in fresh

media. Cells were mixed and co-cultured for different time periods (20,000 cell/100μl treated+20,000 cell/100μl untreated) in media with or without serum. Prior to labelling cells were fixed with paraformaldehyde (PFA) 2% for 15 minutes at room temperature. The PFA was removed (2 x washing) and the cells were resuspended in PBS. Then the CuAAC mix was added. Click solution comprised of 1 mM CuSO4, 100 μM TTMA [(Tris((1-((O-ethyl)carboxymethyl)-(1,2,3-triazol-4-yl))methyl)amine] ligand, and 2 mM sodium ascorbate and 2 μM Alexa Fluor® 647 alkyne (Invitrogen). After 20 minutes, the cells were washed three times with PBS, prior to incubation with 3% bovine serum albumin (BSA) for 30 minutes to remove unreacted fluorophore. The cells were then washed and flow-cytometry was performed. For the cholesterol-alkyne assay, the cells were incubated for 18 hours at 37 °C with 5 μM cholesterol-alkyne 2 (Avanti) in full media[20]. Cells were then co-cultured, fixed and labelled using the above biorthogonal labelling protocol but with 2 μM Alexa Fluor® 488 azide (Invitrogen).

Mammalian cell culture

Cells were cultured in 25 cm^2 flasks and split at 70-80% confluence (three times per week). The flasks were incubated at 37 °C at 7.0% CO_2. The medium was refreshed three times a week. Cells used in all biological experiments were cultured for a maximum of 8 weeks. Adherent cell cultures with a maximum confluence of 70-80% were trypsinised and centrifuged (1.5 mins, 2000/4000 rcf (live/fixed cells), and the cells were resuspended using fresh media. 10 μL of cell suspension and 10 μL of trypan blue were mixed and pipetted into a cell counting slide, and cells were counted using a BioRad TC10 automated cell counter. The cell suspension was diluted to the appropriate seeding density.

HeLa[25], U2Os[27] cells were cultivated in Dulbecco's Modified Eagle's Medium (DMEM), supplemented with 10% foetal calf serum, 2 mM L-glutamine, 1% penicillin and 1% streptomycin. Cells were cultured in an atmosphere of 7% CO_2 at 37 °C. Medium was refreshed every two days and cells passaged at 70% confluence by treatment with trypsin-EDTA (0.05% trypsin). Jurkat[28] 1 and AMO cells were grown in RPMI 1640 medium supplemented with 10% heat-inactivated foetal calf serum, 2 mM L-glutamine, penicillin 100 l.U./mL and streptomycin 50 μg/mL. CTL hybridoma, B3Z[30] was cultured in IMDM medium supplemented with 10% FCS, 2 mM glutamax, 0.25 mM 2-Mercaptoethanol, penicillin 100 l.U./mL and streptomycin 100μg/mL in the presence of hygromycin B (500 μg/ml).[67]

Live cell confocal microscopy

Cells were seeded on a 35 mm dish (3 x 10^5) in a complete media after the addition of 5 μM bdp-Ch 1 for 18 hours. The following day, prior to the confocal microscopy, lipidated coiled-coil peptides were added as follows: 5 μM final concentration of CPE was added to bdp-Ch treated cells and 5 μM of CPK was added to unlabelled cells; both were incubated at 37 °C for 10 minutes. After three washing steps, fresh media was added and cells were transferred into an 8-well μ-slide (Ibidi, cat. 80826) by mixing 1 x 10^4 bdp-Ch-CPE-modified cells with an equal amount of CPK-modified cells per well. Samples were imaged with a Leica TCS SP8 confocal microscope (63x oil lens, N.A.=1.4).

WST-1 cytotoxicity assay[54]

The cell proliferation reagent WST-1 (CAS 150849-52-8) was used to assess cell viability. This assay is based on the cleavage of a tetrazolium salt (WST-1) to soluble formazan dye by the mitochondrial dehydrogenase of living cells. At indicated time-points, 10 ul of a

freshly made mixture of WST-1 and PMS-OMe (90 uM WST-1 and 181 μM PMS-OMe) were added to each well, and the plates were incubated at 37 °C for four hours. Subsequently, the optical densities of the plates were detected at 450 nm (formazan formation) as measured using a 96-well plate reader. The cytotoxicity was expressed as percentage over control.

Transwell assay[68]

Labelled cells were prevented from directly contacting unlabelled cells using a transwell 0.4 μm-pore membrane (Costar). Cells were seeded in a 6-well plate with full DMEM media with or without the addition of 5 μM bdp-cholesterol (TopFLuor®, Avanti) and cells incubated 24h at 37 °C. Cells were detached with 2.5 mM PBS/EDTA, washed and then re-suspended in DMEM media and then counted. Labelled cells (in 0.3 mL of medium) were added in the upper compartment (done in 6-well plates) and unlabelled cells (in 0.5 mL of medium) placed in the lower chamber separated from targets. The inserts were then picked up using gloves and transferred onto the top of the unlabelled HeLa cell culture with the addition of 2 ml of fresh media into the inserts. The cells were incubated for three hours at 37 °C, and then collected and analysed with flow cytometry.

Synthesis of Ac_4ManNAz

Ac_4ManNAz (Tetra-O-Acetyl-N-azidoacetylmannosamine) was synthesised in full accordance with the reported procedure.[56]

^{1}H NMR (400 MHz, $CDCl_3$), δ= 6.04 (d, 1H), 5.91 (d, 1H), 5.49 (d, 1H), 5.33 (d, 1H), 5.18 (dd, 1H), 5.00-4.97 (m, 1H), 4.81 (d, 1H), 4.77 (d, 1H), 4.55 (d, 1H), 4.54 (dd, 1H), 4.52 (d, 1H), 4.4 (m, 2H), 4.32 (m, 7H), 4.1 (m, 1H), 2.14 (s, 3H), 2.11 (s, 3H), 2.04 (s, 6H), 1.99 (s, 6H), 1.5 (s, 3H),

1.34 (s, 3H). LC-MS (ESI): m/z [M+H]+, calc. for $C_{16}H_{22}N_4O_{10}$: 431.37; found 431.37.

Synthesis of peptides

CPE (cholesterol-PEG_{12}-peptideE) and CPK (cholesterol-PEG_{12}-peptideK) were synthesised and purified as previously reported.[39] Peptide sequences were $(EIAALEK)_3$ and $(KIAALKE)_3$ for E and K respectively.

3.5 References

1 C. M. Waters and B. L. Bassler, *Annu. Rev. Cell Dev. Biol.*, 2005, **21**, 319–346.

2 P. H. Raven, G. B. Johnson, J. B. Losos and S. R. Singer, *Biology*, McGraw-Hill Education, New York, 2004.

3 R. C. Lai, F. Arslan, M. M. Lee, N. S. K. Sze, A. Choo, T. S. Chen, M. Salto-Tellez, L. Timmers, C. N. Lee, R. M. El Oakley, G. Pasterkamp, D. P. V de Kleijn and S. K. Lim, *Stem Cell Res.*, 2010, **4**, 214–222.

4 G. Turturici, R. Tinnirello, G. Sconzo and F. Geraci, *Am. J. Physiol. Cell Physiol.*, 2014, **306**, 621–633.

5 X. Niu, K. Gupta, J. T. Yang, M. J. Shamblott and A. Levchenko, *J. Cell Sci.*, 2009, **122**, 600–610.

6 E. Ikonen, *Nat. Rev. Mol. Cell Biol.*, 2008, **9**, 125–138.

7 K. A. Solanko, M. Modzel, L. M. Solanko and D. Wüstner, *Lipid Insights*, 2015, **8**, 95–114.

8 Y. Lange, C. M. Cohen and M. J. Poznansky, *Proc. Natl. Acad. Sci. U. S. A.*, 1977, **74**, 1538–1542.

9 S. Lev, *Nat. Rev. Mol. Cell Biol.*, 2010, **11**, 739–750.

10 J.E. Ferrell Jr, K.J. Lee and W.H. Huestis, *Biochemistry*, 1985, **24**, 2857–2864.

11 L. R. McLean and M. C. Phillips, *Biochemistry*, 1984, **23**, 4624–4630.

12 M. C. Phillips, W. J. Johnson and G. H. Rothblat, *Biochemistry*, 1987, **906**, 223–276.

13 W. A. Prinz, *Prog. Lipid Res.*, 2007, **46**, 297–314.

14 J. T. Crowley, A. M. Toledo, T. J. LaRocca, J. L. Coleman, E. London and J. L. Benach, *PLoS Pathog.*, 2013, **9**, e1003109.

15 M. Mittelbrunn and F. Sánchez-Madrid, *Nat. Rev. Mol. Cell Biol.*, 2012, **13**, 328–335.

16 A. M. Skinner, S. L. O'Neil and P. Kurre, *PLoS One*, 2009, **4**, e6219.

17 M. A. Deverall, E. Gindl, E.-K. Sinner, H. Besir, J. Ruehe, M. J. Saxton and C. A. Naumann, *Biophys. J.*, 2005, **88**, 1875–86.

18 S. Ly, F. Bourguet, N. O. Fischer, E. Y. Lau, M. A. Coleman and T. A. Laurence, *Biophysj*, 2014, **106**, L05–L08.

19 M. Hölttä-Vuori, R. L. Uronen, J. Repakova, E. Salonen, I. Vattulainen, P. Panula, Z. Li, R. Bittman and E. Ikonen, *Traffic*, 2008, **9**, 1839–1849.

20 K. Hofmann, C. Thiele, H.-F. Schött, A. Gaebler, M. Schoene, Y. Kiver, S. Friedrichs, D. Lütjohann and L. Kuerschner, *J. Lipid Res.*, 2014, **55**, 583–591.

21 E. Saxon and C. R. Bertozzi, *Science*, 2000, **287**, 2007–2010.

22 E. M. Sletten and C. R. Bertozzi, *Angew. Chemie - Int. Ed.*, 2009, **48**, 6974–6998.

23 C. Besanceney-Webler, H. Jiang, T. Zheng, L. Feng, D. Soriano del Amo, W. Wang, L. M. Klivansky, F. L. Marlow, Y. Liu and P. Wu, *Angew. Chem. Int. Ed. Engl.*, 2011, **50**, 8051–8056.

24 H. Robson Marsden and A. Kros, *Angew. Chem. Int. Ed. Engl.*, 2010, **49**, 2988–3005.

25 B. D. N. Woolfson, *Advances*, 2005, **70**, 79–112.

26 M. T. Kubicek, G. O. Gey and W. D. Coffman, *Cancer Res.*, 1952, **12**, 264–265.

27 J. Ponten and E. Saksela, *Int. J. Cancer*, 1967, **2**, 434–447.

28 U. Schneider, H. U. Schwenk and G. Bornkamm, *Int. J. Cancer*, 1977, **19**, 621–626.

29 S. Shimizu, T. Takiguchi, M. Fukutoku, R. Yoshioka, Y. Hirose, S. Fukuhara, H. Ohno, Y. Isobe and S. Konda, *Leukemia*, 1993, **7**, 274–280.

30 J. Karttunen and N. Shastri, *Proc. Natl. Acad. Sci.*, 1991, **88**, 3972–3976.

31 B. S. Cummings and R. G. Schnellmann, *Curr. Protoc. Pharmacol.*, 2004, Chapter 12, Unit 12.8.

32 V. P. Torchilin, R. Rammohan, V. Weissig and T. S. Levchenko, *Proc. Natl. Acad. Sci. U. S. A.*, 2001, **98**, 8786–8791.

33 M. Tsubaki, *Biochemistry*, 1993, **32**, 174–182.

34 J. Harvey, S. C. Hardy and M. L. Ashford, *Br. J. Pharmacol.*, 1999, **126**, 51–60.

35 E. C. T. Yeung, C. Stasolla, M. J. Sumner and B. Q. Huang, in *Plant Microtechniques and Protocols*, Springer International Publishing, 2015, 22–43.

36 H. M. Shapiro, *Practical Flow Cytometry*, John Wiley & Sons, New Jersey, Fourth., 2003.

37 J. Iqbal, K. Anwar and M. M. Hussain, *J. Biol. Chem.*, 2003, **278**, 31610–31620.

38 M. K. Herroon, E. Rajagurubandara, D. L. Rudy, A. Chalasani, A. L. Hardaway and I. Podgorski, *Oncogene*, 2013, **32**, 1580–1593.

39 H. R. Zope, F. Versluis, A. Ordas, J. Voskuhl, H. P. Spaink and A. Kros, *Angew. Chem. Int. Ed. Engl.*, 2013, **52**, 14247–14251.

40 F. Versluis, J. Voskuhl, B. Van Kolck, H. Zope, M. Bremmer, T. Albregtse, A. Kros, B. van Kolck, H. Zope, M. Bremmer, T. Albregtse and A. Kros, *J. Am. Chem. Soc.*, 2013, **135**, 8057–8062.

41 L. Kong, S. H. C. Askes, S. Bonnet, A. Kros and F. Campbell, *Angew. Chemie - Int. Ed.*, 2015, **55**, 1396–1400.

42 N. Lopez Mora, A. Bahreman, H. Valkenier, H. Li, T. Sharp, D. N. Sheppard, A. Kros and A. Davis, *Chem. Sci.*, 2016, **7**, 1768–1772.

43 J. Yang, A. Bahreman, G. Daudey, J. Bussmann, R. C. L. Olsthoorn and A. Kros, *ACS Cent. Sci.*, 2016, **2**, 621–630.

44 J. Yang, Y. Shimada, R. C. L. Olsthoorn, B. E. Snaar-Jagalska, H. P. Spaink and A. Kros, *ACS Nano*, 2016, **10**, 7428–7435.

45 G. Charron, *Acc. Chem. Res.*, 2011, **44**, 699–708.

46 X. Zhang and Y. Zhang, *Molecules*, 2013, **18**, 7145–7159.

47 D. M. Patterson, L. A. Nazarova and J. A. Prescher, *ACS Chem. Biol.*, 2014, **9**, 592−605.

48 V. Hong, N. F. Steinmetz, M. Manchester and M. G. Finn, *Bioconjugate Chem.*, 2010, **21**, 1912–1916.

49 C. Uttamapinant, A. Tangpeerachaikul, S. Grecian, S. Clarke, U. Singh, P. Slade, K. R. Gee and A. Y. Ting, *Angew. Chemie - Int. Ed.*, 2012, **51**, 5852–5856.

50 D. Soriano Del Amo, W. Wang, H. Jiang, C. Besanceney, A. C. Yan, M. Levy, Y. Liu, F. L. Marlow and P. Wu, *J. Am. Chem. Soc.*, 2010, **132**, 16893–16899.

51 C. Uttamapinant, M. I. Sanchez, D. S. Liu, J. Z. Yao and A. Y. Ting, *Nat. Protoc.*, 2013, **8**, 1620–1634.

52 L. A. Herzenberg, *Nat. Immunol.*, 2006, **7**, 681–685.

53 G. C. Salzman, S. B. Singham, R. G. Johnston and C. F. Bohren, in *Flow Cytom. Sorting*, Wiley, New York, 1990, 81–107.

54 M. J. Stoddart, *Mamm. Cell Viability Methods Protoc.*, 2011, **740**, 21–25.

55 N. M. Varki and A. Varki, *Lab Invest*, 2007, **87**, 851–857.

56 S. T. Laughlin and C. R. Bertozzi, *Nat. Protoc.*, 2007, **2**, 2930–2944.

57 F. R. Maxfield and D. Wüstner, *Methods Cell Biol.*, 2012, **108**, 367–393.

58 L. Yang, J. O. Nyalwidhe, S. Guo, R. R. Drake and O. J. Semmes, *Mol. Cell. Proteomics*, 2011, **10**, 1–16.

59 D. H. Dube and C. R. Bertozzi, *Nat. Rev. Drug Discov.*, 2005, **4**, 477–488.

60 S. Iyer, R. M. Gaikwad, V. Subba-Rao, C. D. Woodworth and I. Sokolov, *Nat. Nanotechnol.*, 2009, **4**, 389–393.

61 H. Jiang, B. P. English, R. B. Hazan, P. Wu and B. Ovryn, *Angew. Chemie Int. Ed.*, 2015, **54**, 1765–1769.

62 B. D. Levy, C. B. Clish, B. Schmidt, K. Gronert and C. N. Serhan, *Nat. Immunol.*, 2001, **2**, 612–619.

63 M. Winkler, *BJOG An Int. J. Obstet. Gynaecol.*, 2003, **110**, 118–123.

64 M. van der Stelt and V. Di Marzo, *Neuromolecular Med.*, 2005, **7**, 37–50.

65 F. A. Iannotti, V. Di Marzo and S. Petrosino, *Prog. Lipid Res.*, 2016, **62**, 107–128.

66 M. P. Baggelaar, F. J. Janssen, A. C. M. Vanesbroeck, H. Dendulk, M. Allara, S. Hoogendoorn, R. McGuire, B. I. Florea, N. Meeuwenoord, H. Vandenelst, G. A. Vandermarel, J. Brouwer, V. Dimarzo, H. S. Overkleeft and M. Vanderstelt, *Angew. Chemie - Int. Ed.*, 2013, **52**, 12081–12085.

67 G. Cafri, A. Sharbi-Yunger, E. Tzehoval and L. Eisenbach, *PLoS One*, 2013, **8**, 1–7.

68 M. K. Herroon and I. Podgorski, *Bio-protocol*, 2015, **7**, 956–963.